Journal of Global Change Data & Discovery. 2024, 8(1): 21-31
www.geodoi.ac.cn

Global Change Research Data Publishing & Repository

# Dataset for the Reconstruction of Paleofire over 4000 Years in a Typical Profile of the Lubei Plain Region

Zheng, S. X.[1] Tan, Z. H.[1,2]* Mao, L. J. [3] Wang, X. M.[1] Miao, J. H.[1] Lei, Q. J.[1] Yang, L.[1]

1. School of Environmental and Chemical Engineering，Xi'an Polytechnic University，Xi'an 710600，China;
2. State Key Laboratory of Loess and Quaternary Geology，Institute of Earth Environment，Chinese Academy of Sciences，Xi'an 710061，China;
3. School of Marine Science, Nanjing University of Information Science & Technology, Nanjing 210044,China

**Abstract:** This research studies samples collected from a typical terrestrial sediment profile in Changxu Village, Guangrao County, Shandong Province. The research involves indoor analysis on those samples to obtain various environmental proxy data, including Black carbon, Magnetic susceptibility, Loss on ignition, and geochemical elements. Data about climate indices and settlements were collected through GetData software and relevant literature, and combined with chronological data to form a comprehensive dataset. Such dataset analysis primarily involves descriptive statistics and box plots revealing the range and dispersion of data included. Principal component analysis and correlation analysis are employed to interpret meanings represented by different principal components. Furthermore, fire factor scores momentum over different periods are to analyze main controlling factors of fires in various eras. The dataset is stored in .shp and .xlsx formats, consisting of 8 data files, with a total size of 74.3 KB (compressed into one file of 69 KB).

**Keywords: black carbon; Lubei Plain region; Paleofire;Reconstruction; changxu profile; wildfire**

**DOI:** https://doi.org/10.3974/geodp.2024.01.03

**CSTR:** https://cstr.escience.org.cn/CSTR:20146.14.2024.01.03

**Dataset Availability Statement:**

The dataset supporting this paper was published and is accessible through the *Digital Journal of Global Change Data Repository* at: https://doi.org/10.3974/geodb.2024.03.07.V1 or https://cstr.escience.org.cn/CSTR:20146.11.2024.03.07.V1.

**Received:** 12-11-2023; **Accepted:** 26-02-2024; **Published:** 25-03-2024

**Foundations:** National Natural Science Foundation of China (42373085); State Key Laboratory of Loess and Quaternary Geology, Institute of Earth Environment, Chinese Academy of Sciences (SKLLQG22023); Chinese Academy of Sciences (XDB40000000); Science and Technology Department of Shaanxi Province (2023-JC-YB-226)

***Corresponding Author:** Tan, Z. H., School of Environmental and Chemical Engineering，Xi'an Polytechnic University; State Key Laboratory of Loess and Quaternary Geology，Institute of Earth Environment，Chinese Academy of Sciences, tonishtan@163.com.

**Data Citation:** [1] Zheng, S. X., Tan, Z. H., Mao, L. J., *et al*. Dataset for the reconstruction of paleofire over 4000 years in a typical profile of the Lubei Plain region [J]. *Journal of Global Change Data & Discovery*, 2024, 8(1): 21–31. https://doi.org/10.3974/geodp.2024.01.03. https://cstr.escience.org.cn/CSTR:20146.14.2024.01.03.

[2] Zheng, S. X., Tan, Z. H., Mao, L. J., *et al*. Dataset of 4000 years paleofire reconstruction in Lubei Plain [J/DB/OL]. *Digital Journal of Global Change Data Repository*, 2024. https://doi.org/10.3974/geodb.2024.03.07.V1. https://cstr.escience.org.cn/CSTR:20146.11.2024.03.07.V1.

## 1 Introduction

Fires play a critical role in evolution of natural landscapes and carbon cycle from the terrestrial biosphere to the atmosphere[1]. The occurrence of wildfires is closely related to climate change, but over the past 3000 years, human activities have become a significant triggering factor for fires[2]. In recent years, wildfires have happened globally, such as in northeastern Greece, where the largest wildfire recorded in EU took place; Canada has also seen its most severe wildfire season ever; and large-scale fires occurred in the United States and Spain, signaling humanity's entrance into a new "Fire Age". The frequent wildfires are caused by climate change-induced extreme heat, drought, and strong winds, as well as human factors (traffic accidents, intentional arson, etc.). The increasing number of fire events poses significant threats to the ecological environment and human safety, drawing scientific attention.

Currently, many researchers use Black carbon and Charcoal[3–6] in sediments to reconstruct ancient fire events over long timescales. Black carbon refers to a continuum of carbonaceous materials produced by incomplete combustion of biomass or fossil fuels, as well as by weathering of rocks[7]. This spectrum ranges from lightly charred, biodegradable biomass char to highly condensed, fire-resistant soot formed at high temperatures. Due to the complex interactions among climate, tree, and fire, and significant human activities influence on fires under modern conditions, it is challenging to discern these relationships clearly. Additionally, the differences in spatial scales of sampling areas, the variability in Black carbon analysis methods, and the limited precision of single indicators contribute to considerable uncertainties in identifying and quantifying the historical evolution of wildfires. Therefore, utilizing high-resolution Black carbon data, combined with other paleoenvironmental proxies and historical records, can enhance our understanding of interactions among ancient fires, climate, and human activities, which is vital for modern fire prevention and future fire impact assessments.

The stratigraphic profile of the Lubei Plain region has recorded geological and environmental changes over a long time, providing continuous data on environmental changes from prehistory to now. Additionally, this region's unique geographical location at the intersection of the Bohai Sea and the Yellow River is affected by both marine and riverine environments, making it typical in terms of climate, soil types, and their uses. Changxu Village in Guangrao County, located on the North Shandong Plain, possesses a rich cultural history and notable traditional agricultural advantages, endowing it an ideal subject for studying fire activity. This study focuses on the Changxu profile to explore the dominant factors of wildfire activity in different historical periods, aiming athorough analysis on complex mechanisms of wildfires in the area.

## 2 Metadata of the Dataset

The dataset name, authors, geographical region, data year, data publishing and sharing service platform, and data sharing policy of the dataset for the reconstruction of paleofire over 4000 years in a typical profile of the Lubei Plain region[8] are detailed in Table 1.

## 3 Data Development Methods

### 3.1 Research Area

The Changxu profile (118°25′32″E, 37°05′31″N) is located in Changxu Village, Guangrao County, on the Lubei Plain region (Figure 1), a sensitive area of the East Asian monsoon and

**Table 1** Metadata summary of the dataset of 4000 years paleofire reconstruction in Lubei Plain

| Items | Description |
|---|---|
| Dataset full name | Dataset of 4000 years paleofire reconstruction in Lubei Plain |
| Dataset short name | Paleofire&HumanActivities_CX |
| Authors | Zheng, S. X., School of Environmental and Chemical Engineering, Xi'an Polytechnic University, 1207387736@qq.com<br>Tan, Z. H., School of Environmental and Chemical Engineering; Xi'an Polytechnic University, State Key Laboratory of Loess and Quaternary Geology, Institute of Earth Environment, Chinese Academy of Sciences, tonishtan@163.com<br>Mao, L. J., School of Marine Science, Nanjing University of Information Science & Technology, mlj1214@163.com<br>Wang, X. M., School of Environmental and Chemical Engineering, Xi'an Polytechnic University，1767148131@qq.com<br>Miao, J. H., School of Environmental and Chemical Engineering, Xi'an Polytechnic University，miaojihong2021@163.com<br>Lei, Q. J., School of Environmental and Chemical Engineering, Xi'an Polytechnic University，leiqiujing1016@163.com<br>Yang, L., School of Environmental and Chemical Engineering, Xi'an Polytechnic University，995260636@qq.com |
| Geographical region | Lubei Plain region, Shandong Province: Changxu Village, Guangrao County |
| Year | Since 4000 years ago |
| Data format | .shp, .xlsx |
| Data size | 74.3 KB |
| Foundations | National Natural Science Foundation of China (42373085); State Key Laboratory of Loess and Quaternary Geology, Institute of Earth Environment, Chinese Academy of Sciences (SKLLQG22023); Chinese Academy of Sciences (XDB40000000); Science and Technology Department of Shaanxi Province (2023-JC-YB-226) |
| Data publisher | Global Change Research Data Publishing & Repository, http://www.geodoi.ac.cn |
| Address | No. 11A, Datun Road, Chaoyang District, Beijing 100101, China |
| Data sharing policy | (1) *Data* are openly available and can be free downloaded via the Internet; (2) End users are encouraged to use *Data* subject to citation; (3) Users, who are by definition also value-added service providers, are welcome to redistribute *Data* subject to written permission from the GCdataPR Editorial Office and the issuance of a *Data* redistribution license; and (4) If *Data* are used to compile new datasets, the 'ten per cent principal' should be followed such that *Data* records utilized should not surpass 10% of the new dataset contents, while sources should be clearly noted in suitable places in the new dataset[9] |
| Communication and searchable system | DOI, CSTR, Crossref, DCI, CSCD, CNKI, SciEngine, WDS/ISC, GEOSS |

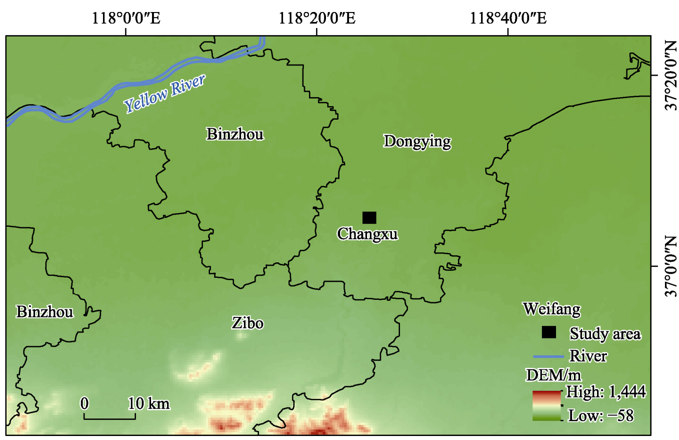


**Figure 1** Map of the study area and sampling points

characterized by temperate continental monsoon climate. It features rainy and humid summers and dry winters with precipitation and heat simultaneously, prone to trigger natural disasters such as droughts, floods, and salinization; the terrain is predominantly plains, with hills and low hill zones. This region enjoys cultural relics of long history, among which the Yueshi culture and Shang-Zhou culture are famous. The Yueshi culture, a prehistoric culture from the late Neolithic to the early Bronze Age in China, is characterized by stone tools usage, demonstrating ancient human activities such as hunting, gathering, and tool-making. The Shang-Zhou culture represents an important stage in ancient Chinese civilization, during which ancient people developed agriculture, handicrafts, and commerce, promoting local society.

### 3.2 Data Source

The paleoenvironmental proxy data included are derived from indoor laboratory analyses following field sampling and relevant literature (Table 2). The raw data for Magnetic susceptibility, Loss on ignition, Black carbon concentration, and geochemical elements were collected by measuring and calculating via respective experimental methods. The GetData software was employed to acquire ice core oxygen isotope $\delta^{18}O$, Temperature Index from Phytolith, cave stalagmite $\delta^{18}O$, and tree data from relevant literature. Population data were gathered from related literature and books. Additionally, the chronological framework of this study profile[10] is based on OSL dating data of the Changxu profile sediments, stratigraphic divisions, and archaeological information from cultural relics.

**Table 2** Methods for collecting paleoenvironmental proxy data

| number | Indicator | Data acquisition methods | Data source |
|---|---|---|---|
| 1 | Magnetic susceptibility | Magnetic susceptibility was measured using an MS-2B type magnetometer (0.47/4.7 kHz) manufactured by Bartington Instruments, UK | This study |
| 2 | Loss on ignition | Take 0.4 g of each sample and place it in a porcelain crucible in a muffle furnace (X-5-12 model) of known mass. Burn at 900 °C for 2 hours and weigh the residue for measurement | This study |
| 3 | Black carbon | Measured using a DRI2001 model OC/EC carbon analyzer from the United States, employing the thermal/optical reflectance (TOR) method | This study |
| 4 | Mn | Geochemical elements were measured using a PW2403 X-Ray fluorescence spectrometer at the Institute of Earth Environment, Chinese Academy of Sciences | This study |
| 5 | P | | This study |
| 6 | Ti | | This study |
| 7 | Rb | | This study |
| 8 | Sr | | This study |
| 9 | Ice Core Oxygen Isotope $\delta^{18}O$ | Obtained using GetData software | [11] |
| 10 | Temperature Index from Phytolith | Obtained using GetData software | [12] |
| 11 | Shandong cave $\delta^{18}O$ | Obtained using GetData software | [13] |
| 12 | Tree | Obtained using GetData software | [14] |
| 13 | Settlements | Historical literature, relevant books | [15–17] |

### 3.2 Principles of Data Analysis

**3.2.1** Correlation Analysis

Correlation analysis is commonly employed to measure the strength and direction of relationships between two or more variables, illustrating hidden patterns and correlations and thereby enhancing our understanding about them within the data. This article employs correlation analysis to quantify the relationships between Rb/Sr, Mn, Ti, Loss on ignition, Soot, Char, settlements, and Temperature Index from Phytolith, reflecting the interrelationships among multiple variables.

**3.2.2** Principal Component Analysis

Principal component analysis (PCA) is a multivariate statistical method that simplifies multiple variables into a few representative composite variables, allowing a more intuitive observation of the overall differences between various samples. PCA aims to reduce the dimensionality of a dataset while retaining as much of the variability or information from the original data as possible, facilitating subsequent analyses. Loadings are an important aspect of PCA; the greater the absolute loading value, the greater the contribution of that feature to the principal component. If a particular principal component has high loadings for certain features and low loadings for others, this principal component can be viewed as a “theme” related to these high-loading features, promoting understanding about meaning represented by each principal component. In this dataset, PCA is employed to identify the key factors influencing fire incidents across different periods and their contributions. On top of that, scatter plots and Sankey diagrams are utilized to visualize the results, more intuitively illustrating the relationships between principal components and samples distribution in the principal component space.

# 4 Data Results and Validation

## 4.1 Data Composition

The dataset contains following data from the Changxu profile: (1) geographic locations of sampling points; (2) age, depth, and sedimentation rates; (3) low-frequency magnetic susceptibility; (4) loss on ignition; (5) concentrations of soot, char, and black carbon; (6) geochemical elements; (7) multiple climate indicators; (8) principal component analysis data.

## 4.2 Data results

**4.2.1** Descriptive Statistics of Different Paleoenvironmental Proxy Indicators

Table 3 indicates that the concentrations of Char, Soot, and Black carbon in the Changxu profile respectively range between 0.042–0.709 $mg·g^{-1}$, 0.011-0.299 $mg·g^{-1}$, and 0.087–0.904 $mg·g^{-1}$. Low-frequency Magnetic susceptibility and Loss on ignition respectively fluctuate between $35.870×10^{-8}$–$141.200×10^{-8}$ $m^3·kg^{-1}$ and 0.038%–0.099%. The contents of Mn, Ti, P, and the Rb/Sr ratio respectively vary between 386.45–1,031.52 ppm, 3,368.11–4,767.82 ppm, 393.75–750.21 ppm, and 0.477–0.983. Combined with the box plots (Figure 2) of the Changxu profile across four time periods[10], the concentrations of Black carbon, Char, and Soot, the contents of Mn, P, Ti, Loss on ignition, Magnetic susceptibility, and the Rb/Sr ratio are mostly within the 1.5 IQR reasonable range, indicating that the dataset is concentrated with few outliers, and indicator variables distribution is relatively uniform. This not only demonstrates the data stability and reliability but also lays a solid foundation for further statistical analysis.

**Table 3** Descriptive statistics table for different environmental proxy indicators

| indicator | Char ($mg·g^{-1}$) | Soot ($mg·g^{-1}$) | Black carbon ($mg·g^{-1}$) | Low-frequency Magnetic susceptibility ($10^{-8}$ $m^3·kg^{-1}$) | Loss on ignition (%) | Rb/Sr | Mn (ppm) | Ti (ppm) | P (ppm) |
|---|---|---|---|---|---|---|---|---|---|
| Maximum value | 0.709 | 0.299 | 0.904 | 141.200 | 0.099 | 0.983 | 1,031.52 | 4,767.82 | 750.21 |
| minimum value | 0.042 | 0.011 | 0.087 | 35.870 | 0.038 | 0.477 | 386.45 | 3,368.11 | 393.75 |
| mean | 0.368 | 0.102 | 0.470 | 83.017 | 0.067 | 0.617 | 640.24 | 4,096.95 | 530.14 |
| standard deviation | 0.153 | 0.052 | 0.188 | 22.209 | 0.013 | 0.122 | 139.23 | 262.63 | 88.58 |

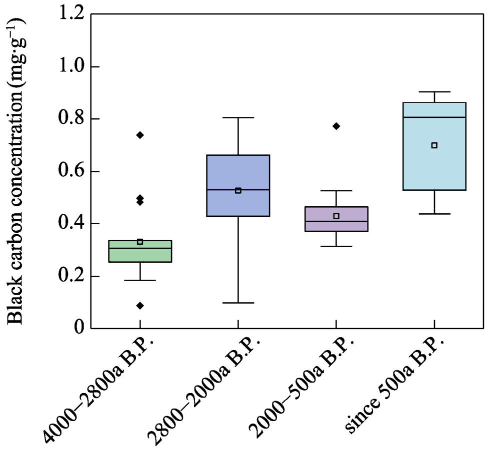


**Figure 2 (a)** Box plot of Black carbon concentration in the Changxu profile

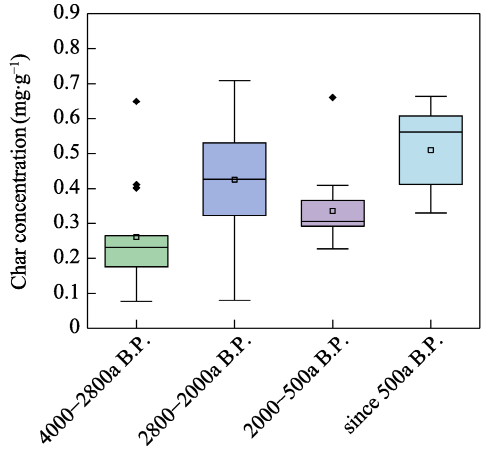


**Figure 2 (b)** Box plot of Char concentration in the Changxu profile

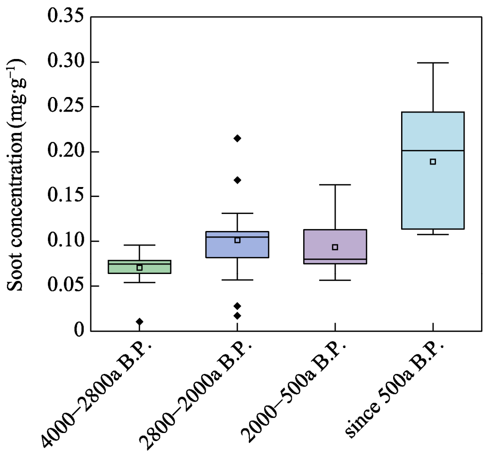


**Figure 2 (c)** Box plot of Soot concentration in the Changxu profile

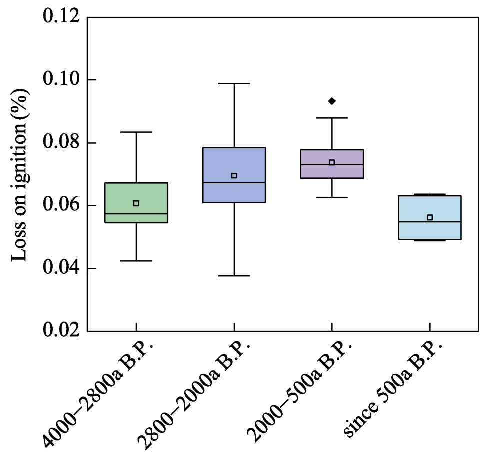


**Figure 2 (d)** Box plot of Loss on ignition in the Changxu profile

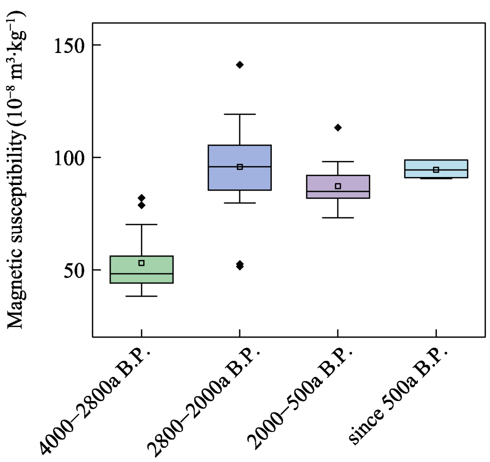


**Figure 2 (e)** Box plot of Magnetic susceptibility in the Changxu profile

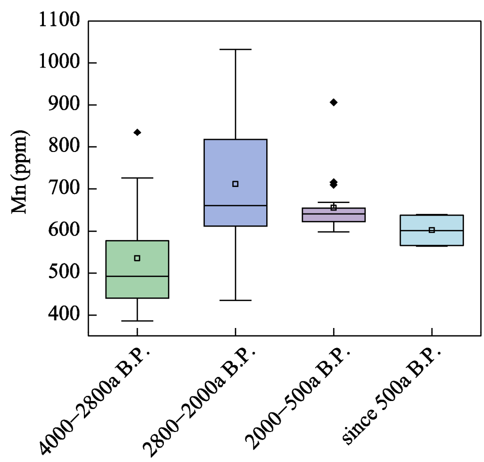


**Figure 2 (f)** Box plot of Mn content in the Changxu profile

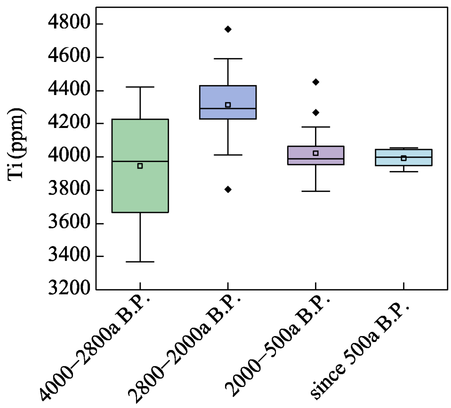


**Figure 2 (g)** Box plot of Ti content in the Changxu profilea

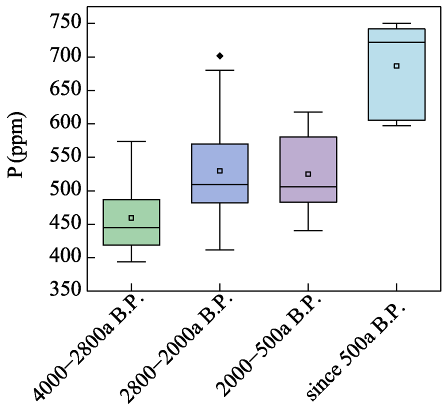


**Figure 2 (h)** Box plot of P content in the Changxu profile

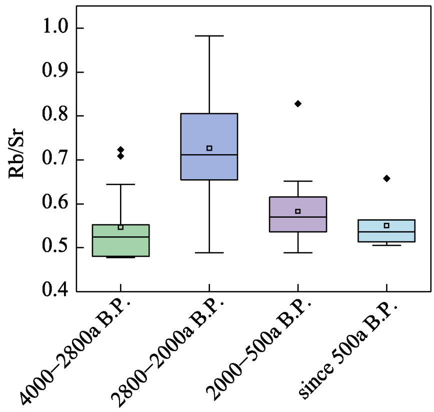


**Figure 2 (i)** Box plot of Rb/Sr in the Changxu profile

### **4.2.2** Correlation Analysis Results

Table 4 indicates a significant correlation between Rb/Sr, Mn, Ti, and Loss on ignition, suggesting that these indicators may reflect similar or interconnected geological or environmental processes. Similarly, the significant correlations between Char, Soot, and settlements indicate a close relationship between Soot and Char and human activities. However, the correlation between Soot and Rb/Sr, Ti, Loss on ignition is not significant, indicating that geological background and soil chemical properties changes have little impact on Soot deposition. The correlation between Temperature Index from Phytolith and other indicators is also not significant, which may suggest that the paleoclimate changes reflected by phytolith temperature are relatively independent from the environmental or

**Table 4** Correlation of Soot and Char with other indicators in the Changxu profile

| | Rb/Sr | Mn | Ti | Loss on ignition | Soot | Char | settlements | Temperature Index from Phytolith |
|---|---|---|---|---|---|---|---|---|
| Rb/Sr | 1.00 | 0.883** | 0.831** | 0.678** | 0.130 | 0.589** | 0.375** | 0.038 |
| Mn | | 1.00 | 0.770** | 0.797** | 0.291* | 0.667** | 0.485** | 0.076 |
| Ti | | | 1.00 | 0.520** | 0.155 | 0.536** | 0.355** | –0.227 |
| Loss on ignition | | | | 1.00 | 0.075 | 0.438** | 0.311* | 0.244 |
| Soot | | | | | 1.00 | 0.567** | 0.380** | –0.137 |
| Char | | | | | | 1.00 | 0.443** | –0.063 |
| settlements | | | | | | | 1.00 | 0.061 |
| Temperature Index from Phytolith | | | | | | | | 1.00 |

*. Significant at the 0.05 level.
**. Significant at the 0.01 level (two-tailed).

human activities within the study area. Those correlation analysis results can offer important references for factor categorization in principal component analysis.

**4.2.3** Principal Component Analysis Results

Using SPSS 27 for principal component analysis, the KMO value is 0.740 (>0.5), indicating good suitability for factor analysis. Principal component analysis was performed through variables from sediments including Rb/Sr, Mn, Ti, Loss on ignition, Soot, Char, Temperature Index from Phytolith, and the social indicator of settlements. Extract three principal components (Figure 3).

PC1 (Principal Component 1) represents the greatest variation's direction within the dataset, in which the data distribution points is of broadest, thereby capturing the most significant momentum that likely represents the most influential factors within the data. In this principal component analysis, PC1 accounts for 43.372% of the variance contribution, comprising Rb/Sr, Mn, Ti, and Loss on ignition (Figure 4), with loadings of 0.931, 0.906, 0.869, and 0.809 respectively. The concentrations of Mn and Ti reflect the bioprocessing intensity during soil formation under anhydrous saturated oxidative conditions. The enrichment of Mn and Ti occurs during intense bioprocessing in soil formation process, mainly caused by a warm and humid environment associated with monsoonal climate changes. Moreover, Mn and Ti are essential elements for Tree, enriched through the decay of plant material within soil. Loss on ignition reflects the content of organic carbon in soil and tree cover. The significant correlation among Rb/Sr, Mn, Ti, and Loss on ignition (Table 4) suggests that PC1 indicates Tree (humidity).

PC2 (Principal Component 2) represents the direction of the second greatest variation in the dataset, orthogonal (i.e., independent) to PC1. PC2 depicts the secondary momentum beyond the variance explained by PC1. Therefore, PC2 may represent the second most important influencing factor in the data. In this principal component analysis, PC2 accounts for 23.870% of the variance contribution, comprising Soot, Char, and settlements (Figure 4), with loadings of 0.910, 0.697, and 0.649 respectively. Char and Soot respectively reflect regional occurrences of wildfires and broader scale biomass burning conditions, while settlements indicate the population's size and scale. The significant correlations among Char, settlements, and Soot, but not between Soot and other climatic indicators (Table 4), suggest that PC2 can indicate anthropogenic fires closely related to population size and biomass burning.

PC3 (Principal Component 3) represents the third largest direction of variation in the dataset, orthogonal to the plane defined by PC1 and PC2. Similarly, it reflects the third most important momentum in the data. In this principal component analysis, PC3 accounts for 14.994% of the variance contribution, primarily composed of Temperature Index from Phytolith (Figure 4), with a loading of 0.961. Temperature Index from Phytolith can indicate

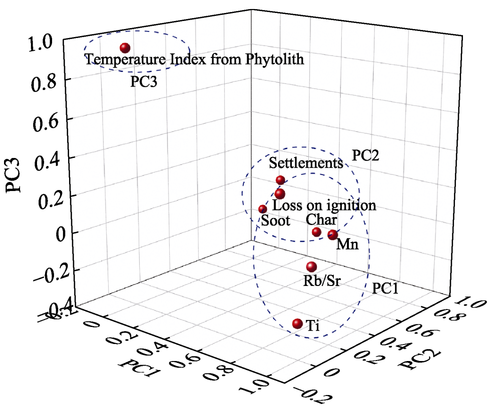


**Figure 3** Principal component analysis results diagram

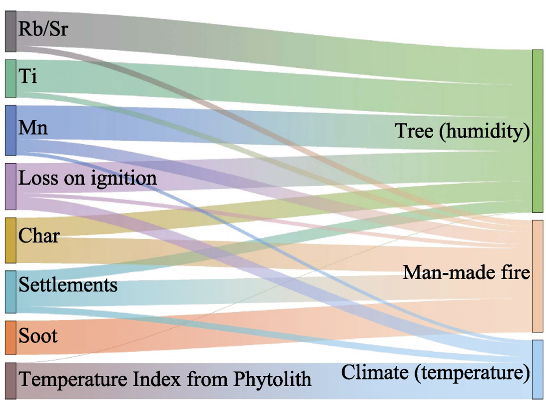


**Figure 4** Sankey diagram

climatic warmth and serves as an ideal proxy for past environmental temperature changes. The correlation of Temperature Index from Phytolith with other indicators is not significant (Table 4), indicating that PC3 can represent temperature related to climate changes.

The curve diagram of fire factor scores over time (Figure 5) shows that this area experienced a generally warmer climate from 4000 to 2800 a B.P., with lower Black carbon values. However, as the climate cooled and a high flood period arrived around 3000 years ago, climate (temperature) and tree (humidity) have been suggested to be the main influencing factors. During the 2800 to 2000 a B.P. period, climate there was generally warm and dry, providing favorable conditions for fire occurrences, with higher Black carbon values. The Spring and Autumn through the Warring States periods, have seen a continual development of human agricultural activities and increased land use, indicating that human activities had a gradually intensifying impact on fire occurrences even tree (humidity) remained a critical precondition for fires. From 2000 to 500 a B.P., the overall climate was cooler and drier, with relatively lower Black carbon values, again highlighting the decisive impact of climate (temperature) on wildfire occurrences. Since 500 a B.P., the climate became further arid, and during the Ming and Qing dynasties, human civilization rapidly developed with increasing fire usage intensity, making frequent human activities the dominant factor in fire events.

The principal factors influencing fire occurrence in the study area over the past 4000 years can be categorized into three main groups: Tree (humidity), human activity, and climate (temperature). Moreover, the primary factors affecting fire occurrence have varied significantly across different time periods.

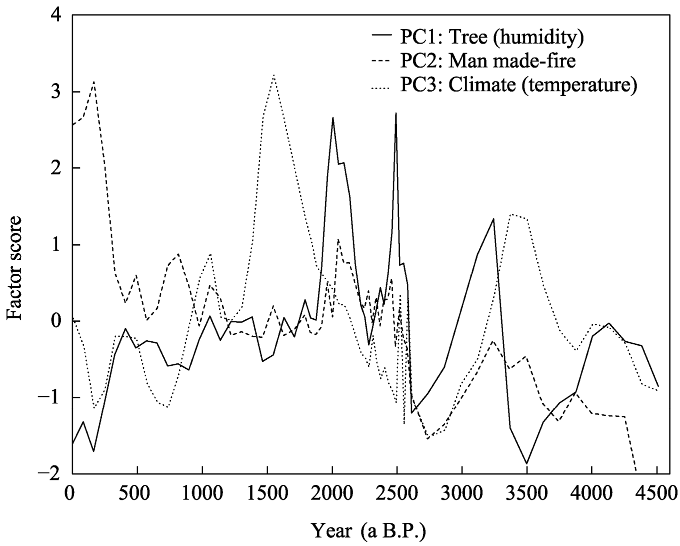


**Figure 5** Curve diagram of fire factor scores over time

### 4.3 Data Validation

**4.3.1** Indoor Experimental Analysis

Ensuring the accuracy and reliability of the experiment is crucial when conducting indoor experiments. Therefore, this study implemented quality control measures, mainly including the following aspects:

(1) Use of blank samples

Blank samples for Black carbon, Magnetic susceptibility, Loss on ignition, and geochemical elements are introduced to check for external contamination or errors introduced by laboratory conditions, reagents, or instruments, ensuring the data purity and the experimental results validity.

(2) Analysis of duplicate samples

In the measurement process of Black carbon, Magnetic susceptibility, and Loss on ignition, one sample is randomly selected from every ten samples for duplicate testing to ensure the relative error within 10%.

(3) National soil reference material samples

While measuring geochemical elements, national standard soil reference material samples are used to calibrate the analysis results and ensure that the measurement error is kept below 5%.

**4.3.2** GetData Data Extraction

Before extracting data, it is essential to clearly define the type and scope of required data, and to choose data sources highly relevant and reliable. When extracting data, select appropriate methods to ensure data extraction accuracy and consistency.

(1) Ensuring the reliability of data sources

While selecting data sources, this study chooses data from articles published in academic journals and official published books.

(2) Ensuring the accuracy and reliability of the data extraction process

When using GetData software for data extraction, the file import extraction method is chosen for precise data points. After extracting, compare the data extracted by GetData software with the original data source to ensure consistency and more accurate utilization of the required data.

## 5 Discussion and Conclusion

This study selected a typical continental sedimentary profile from Changxu Village in Shandong Province as the research subject. Through precise laboratory analysis and stringent quality control measures, including blank samples, duplicate sample analysis, and comparison with national soil reference material samples, the data accuracy of black carbon, Magnetic susceptibility, Loss on ignition, and geochemical elements was ensured. Depending on the GetData software's efficiency in data extraction, data were imported from reliable sources, ensuring the extraction accuracy and source consistency of data. Based on various paleoenvironmental proxy indicators and employing principal component analysis and correlation analysis, the study revealed the main controlling factors for wildfires in the region during different periods. Multivariate statistical analysis results indicate that from 4000 to 2800 a B.P., climate (temperature) and Tree (humidity) were the main influencing factors; from 2800 to 2000 a B.P., human activities increasingly impacted fire occurrences, though Tree (humidity) remained a critical prerequisite for fires; from 2000 to 500 a B.P., climate (temperature) had a decisive impact on wildfires; and since 500 a B.P., increasingly frequent human activities have become the dominant factor in fire events. The research results not only deepen the understanding of the complex mechanisms and key controlling factors of regional wildfires but also lay a foundation for sustainable development amid the background of global warming and climate change.

***Author Contributions***

Zheng, S., X. processed the data and wrote the data paper. Tan, Z. H. designed the overall development of the dataset; Mao, L. J. provided soil samples and OSL dating data; Wang, X. M., Miao, J. H., and Lei, Q. J. conducted data collection. Yang, L. performed data validation.

***Conflicts of Interest***

The authors declare no conflicts of interest.

## References

[1] Bowman, D., Balch, J., Artaxo, P., *et al*. Fire in the earth system [J]. *Science*, 2009(324): 481–484.

[2] Marlon, R. J., Bartlein, P. J., Daniau, A. L., *et al*. Global biomass burning: a synthesis and review of Holocene paleofire records and their controls [J]. *Quaternary Science Reviews*, 2013(65): 5–25.

[3] Chen, T. Z. Distribution characteristics of Black carbon in subarctic Pacific sediments and the reconstruction of late Quaternary paleo-wildfires [D]. Jinan: Shandong University, 2023.

[4] Zhang, Z., Zhao, Y. J., Liu, C. F., *et al*. Response of fire to vegetation and climate change during the Pliocene-Pleistocene in the Nihewan Basin [J]. *Quaternary Sciences*, 2024, 44(1): 16–28.

[5] Song, Y. Q. Charcoal characteristics in the Xiashu Loess of Yangzhou area and their paleoenvironmental implications [D]. Shanghai: East China Normal University, 2024.

[6] Brugger, S., Mcwethy, D., Chellman, N. Holocene Black carbon in New Zealand lake sediment records [J]. *Quaternary Science Reviews*, 2024(325): 108491.

[7] Jiang, S. S., Zhao, D. B., Tang, Y., *et al*. Application of Black carbon in sediment for paleoenvironmental and paleoclimatic studies [J]. *Marine Geology and Quaternary Geology*, 2023, 43(5): 119–135.

[8] Zheng, S. X., Tan, Z. H., Mao, L. J., *et al*. Dataset of 4000 years paleofire reconstruction in Lubei Plain [J/DB/OL]. *Digital Journal of Global Change Data Repository*, 2024. https://doi.org/10.3974/geodb.2024.03.07.V1. https://cstr.escience.org.cn/CSTR:20146.11.2024.03.07.V1.

[9] GCdataPR Editorial Office. GCdataPR data sharing policy [OL]. https://doi.org/10.3974/dp.policy.2014.05 (Updated 2017).

[10] Wang, X. M., Tan, Z. H., Miao, J. H., *et al*. Reconstruction of Paleofire and human activities in typical section of the Lubei Plain area since nearly 4000 years. [J] *Journal of Arid Land Resources and Environment*, 2023, 37(11): 92–99.

[11] Kawamura, K., Parrenin, F., Lisiecki, L., *et al.* Northern hemisphere forcing of climatic cycles in Antarctica over the past 360,000 years [J]. *Nature*, 2007, 448(7156): 912–916.

[12] Nan, X. L., Du, J., Li, P. Y., *et al*. Characteristics of phytoliths in a core near Dongying Harbor and their paleo-environmental implications [J]. *Advances in Marine Science*, 2015, 33(3): 385–393.

[13] Dong, J., Wang, Y., Cheng, H., *et al*. A high-resolution stalagmite record of the Holocene East Asian monsoon from Mt Shennongjia, central China [J]. *The Holocene*, 2010, 20(2): 257–264.

[14] Yang, S., Song, B., Ye, S., *et al*. Large-scale pollen distribution in marine surface sediments from the Bohai Sea, China: Insights into pollen provenance, transport, deposition, and coastal-shelf paleoenvironment [J]. *Progress in Oceanography*, 2019, 178: 102183.

[15] Goldewijk, K., Beusen, A., Doelman, J., *et al*. Anthropogenic land use estimates for the Holocene-HYDE 3.2 [J]. *Earth System Science Data*, 2017, 9(2): 927–953.

[16] Wan, J. H. A study of prehistoric populations in the middle and lower reaches of the Yellow River [D]. Jinan: Shandong University, 2005.

[17] Wu, Y. L. Chinese Population (Shandong Rite) [M]. Beijing: China Financial and Economic Publishing House, 1989.